J|A|C|S ARTICLES

Published on Web 03/26/2009

Synthesis and Structural Characterization of Sialic Acid−Glutamic Acid Hybrid Foldamers as Conformational Surrogates of α-2,8-Linked Polysialic Acid

Jonel P. Saludes, James B. Ames, and Jacquelyn Gervay-Hague*

Department of Chemistry, University of California, One Shields Avenue, Davis, California 95616

Received October 21, 2008; E-mail: gervay@chem.ucdavis.edu

Abstract: Surface expression of α-(2,8)-linked polymers of sialic acid in adult tissues has been correlated with metastasis of several human cancers. One approach to chemotherapeutic intervention against the spread of these cancers involves the development of immunogenic molecules that elicit an antibody response against α-(2,8)-linked polysialic acids. Naturally occurring polysialic acids are not viable candidates because they are present during embryonic development and are recognized as self by the immune system. These natural polymers also have poor pharmacokinetic properties because they are readily degraded by neuraminidase enzymes. We have been interested in developing structural surrogates of polysialic acids in an effort to overcome these limitations. Reported herein are microwave-assisted solid-phase peptide syntheses and structural characterization studies of a series of α/δ hybrid peptides derived from Fmoc−Neu2en and Fmoc−Glu(O*t*Bu)−OH. Conformational experiments including circular dichroism, NH/ND exchange, and ROESY in aqueous solution were performed to study the secondary structures of these hybrid foldamers. ROESY data were analyzed with the assistance of XPLOR-NIH that was modified to include parameter and topology files to accommodate unnatural amino acids and the δ amide linkages. The results indicate that stable secondary structure is dependent upon both the amino acid sequence and the configuration of Glu. The most stable foldamer was composed of a total of 6 residues beginning with L-Glu at the carboxy terminus and alternating Neu2en and L-Glu residues. In water, this foldamer adopts a right-handed helical conformation with 3.7 residues per turn, 7.4 Å pitch, 5.8 Å diameter, and a length of 18.5 Å, which is stabilized by both classical C═O···H−N backbone interactions and by pyranose ring *O* and L-Glu HN H-bonding. These structural features orient the L-Glu carboxylates along the helical backbone with a periodicity that matches the carboxylate positions along the reported G2$^+$ left-handed helix of α-(2,8)-polysialic acid. However, the charge density of the foldamer is one-half that of the natural polymer. These findings provide a fundamental understanding of the factors that influence stable secondary structure in hybrid Neu2en/Glu systems, and the tools we have developed establish a viable platform for the rational design of α-(2,8)-polysialic acid surrogates.

Introduction

Significant advances in the rational design and synthesis of peptide mimetics have been achieved in recent years. Many of the developments in this area have addressed some of the pharmacological limitations of naturally occurring biologically active peptides, for example, enzymatic hydrolysis. A field of unnatural peptide research has emerged, called foldamer science,[1] that addresses not only the problem of proteolysis,[2,3] but also provides a platform for the mimicry of secondary (2°) structures like helices, sheets, and turns,[4−10] and higher order helical bundles found in natural peptides.[11,12] These unnatural peptides can also act as scaffolds with sophisticated biological functions that include antibacterial magainin mimetics[13,14] as well as inhibitors of protein−protein interactions[15,16] and viral infections.[17,18] In a recent review, developments in structural characterization and in vitro and in vivo evaluation of foldamers document the extensive chemotherapeutic potential and diversity of cyclic and acyclic peptide backbones derived from natural and unnatural amino acids.[19]

(1) Gellman, S. H. *Acc. Chem. Res.* **1998**, *31*, 173–180.
(2) Frackenpohl, J.; Arvidsson, P. I.; Schreiber, J. V.; Seebach, D. *ChemBioChem* **2001**, *2*, 445–455.
(3) Disney, M. D.; Hook, D. F.; Namoto, K.; Seeberger, P. H.; Seebach, D. *Chem. Biodiversity* **2005**, *2*, 1624–1634.
(4) Seebach, D.; Abele, S.; Gademann, K.; Guichard, G.; Hintermann, T.; Jaun, B.; Matthews, J. L.; Schreiber, J. V. *Helv. Chim. Acta* **1998**, *81*, 932–982.
(5) Appella, D. H.; Christianson, L. A.; Karle, I. L.; Powell, D. R.; Gellman, S. H. *J. Am. Chem. Soc.* **1996**, *118*, 13071–13072.
(6) Peelen, T. J.; Chi, Y.; English, E. P.; Gellman, S. H. *Org. Lett.* **2004**, *6*, 4411–4414.
(7) Wang, X.; Espinosa, J. F.; Gellman, S. H. *J. Am. Chem. Soc.* **2000**, *122*, 4821–4822.
(8) Seebach, D.; Hook, D. F.; Glattli, A. *Biopolymers* **2006**, *84*, 23–37.
(9) Hanessian, S.; Luo, X.; Schaum, R.; Michnick, S. *J. Am. Chem. Soc.* **1998**, *120*, 8569–8570.
(10) Smith, M. D.; Claridge, T. D. W.; Tranter, G. E.; Sansom, M. S. P.; Fleet, G. W. J. *Chem. Commun.* **1998**, *18*, 2041–2042.
(11) Goodman, J. L.; Petersson, E. J.; Daniels, D. S.; Qiu, J. X.; Schepartz, A. *J. Am. Chem. Soc.* **2007**, *129*, 14746–14751.
(12) Horne, W. S.; Price, J. L.; Gellman, S. H. *Proc. Natl. Acad. Sci. U.S.A.* **2008**, *105*, 9151–9156.
(13) Som, A.; Vemparala, S.; Ivanov, I.; Tew, G. N. *Biopolymers* **2008**, *90*, 83–93.

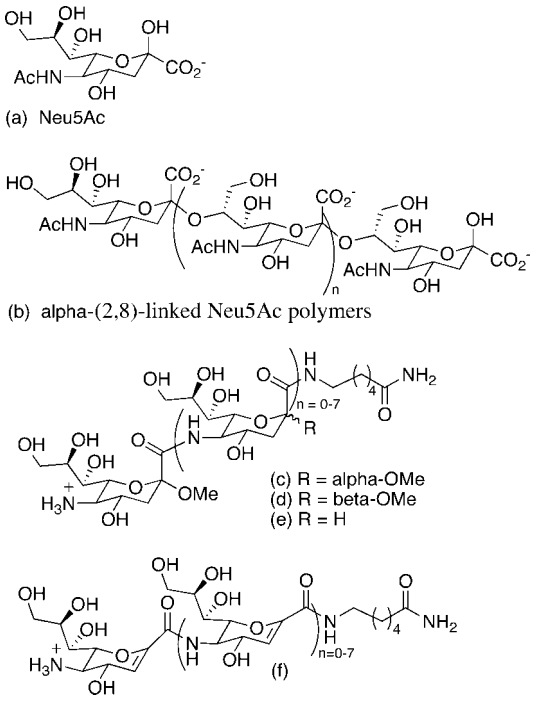

Figure 1. Sialic acid and its natural and synthetic homo-oligomers.

Sugar amino acids (SAAs) are carbohydrates that possess amino and carboxylic acid groups, and they serve as novel foldamer building blocks consisting of an amino acid functionality and a rigid sugar pyran framework with desirable water solubility properties.[20] Sialic acid (Neu5Ac, Figure 1a) is a naturally occurring nine-carbon pyranose SAA that is typically found as a terminal sugar of oligosaccharides attached to proteins and lipids. These sugar chains decorate mammalian cell surfaces and impart profound effects upon human physiology and pathology.[21] In humans, α-(2,8)-linked Neu5Ac polymers (Figure 1b) post-translationally modify neural cell adhesion molecules (N-CAMs) primarily during embryonic development. N-CAMs are a class of high molecular weight cell surface sialoglycoproteins that function in cell adhesion and cell movement.[22−24] Embryonic N-CAM is characterized by a high Neu5Ac content and undergoes a postnatal conversion to the adult form of N-CAM with a low Neu5Ac content.[24,25] Cellular adhesion is reduced in embryonic cells presumably due to charge repulsion between the polyanionic structures, which facilitates cellular migration. In contrast, adhesion is promoted between cells expressing the adult form of N-CAM, which helps stabilize adult tissues.

Interestingly, surface expression of Neu5Ac polymers in adult tissues has been correlated with metastasis of several human tumors, making this polymer a viable candidate for chemotherapeutic intervention.[26−29] Because Neu5Ac polymers are not present in healthy adult tissues, except for localized regions of the brain,[30−34] antibody-based approaches provide a means for selectively targeting cancer cells with high Neu5Ac content. This strategy requires the design and synthesis of molecules that when administered to a patient would elicit an immune response that results in the production of antibodies cross-reactive with Neu5Ac polymers. Conventional wisdom suggests that natural Neu5Ac polymers would not be viable candidates because they are seen as self by the immune system.

Our interest in foldamer science has been motivated by the challenge of developing structural surrogates of Neu5Ac polymers with the long-term objective of developing smaller constructs with stable secondary structure and improved bioavailability profiles. Over a decade ago, our program began with a very simple question: How would the structures of amide-linked Neu5Ac foldamers compare to glycosidically linked oligomers?[35−38] From the early work of Jennings[39] and Yamasaki,[40] we were aware that decamers of α-(2,8)-linked Neu5Ac form stable helical structures. At the outset, we did not expect *O*-linked and amide-linked Neu5Ac polymers to have the same 2° structures; in fact, we were not even sure that amide-linked analogues would be water soluble. Therefore, our initial studies focused on developing methods for the synthesis of amide-linked oligomers and reliable tools for studying their structural properties. We reported the first Neu5Ac-based unnatural synthetic foldamers that form stable 2° structures in water (Figure 1c−f).[41,42] These constructs were primarily characterized by analysis of circular dichroism (CD) studies, which demonstrated that a minimum of 4 residues are required for ordered structure, and further elongation to eight residues increases 2° structure stability. This feature is in contrast to

(14) Schmitt, M. A.; Weisblum, B.; Gellman, S. H. *J. Am. Chem. Soc.* **2004**, *126*, 6848–6849.
(15) Sadowsky, J. D.; Fairlie, W. D.; Hadley, E. B.; Lee, H. S.; Umezawa, N.; Nikolovska-Coleska, Z.; Wang, S. M.; Huang, D. C. S.; Tomita, Y.; Gellman, S. H. *J. Am. Chem. Soc.* **2007**, *129*, 139–154.
(16) Kritzer, J. A.; Stephens, O. M.; Guarracino, D. A.; Reznik, S. K.; Schepartz, A. *Bioorg. Med. Chem. Lett.* **2005**, *13*, 11–16.
(17) Akkarawongsa, R.; Potocky, T. B.; English, E. P.; Gellman, S. H.; Brandt, C. R. *Antimicrob. Agents Chemother.* **2008**, *52*, 2120–2129.
(18) Stephens, O. M.; Kim, S.; Welch, B. D.; Hodson, M. E.; Kay, M. S.; Schepartz, A. *J. Am. Chem. Soc.* **2005**, *127*, 13126–13127.
(19) Bautista, A. D.; Craig, C. J.; Harker, E. A.; Schepartz, A. *Curr. Opin. Chem. Biol.* **2007**, *11*, 685–692.
(20) Von Roedern, E. G.; Kessler, H. *Angew. Chem., Int. Ed. Engl.* **1994**, *33*, 687–689.
(21) Varki, A. *Trends Mol. Med.* **2008**, *14*, 351–360.
(22) Cunningham, B. A.; Hemperly, J. J.; Murray, B. A.; Prediger, E. A.; Brackenbury, R.; Edelman, G. M. *Science* **1987**, *236*, 799–806.
(23) Rutishauser, U.; Acheson, A.; Hall, A. K.; Mann, D. M.; Sunshine, J. *Science* **1988**, *240*, 53–57.
(24) Hoffmann, S.; Sorkin, B. C.; White, P. C.; Brackenbury, R.; Mailhammer, R.; Rutishauser, U.; Cunningham, B. A.; Edelman, G. M. *J. Biol. Chem.* **1982**, *257*, 7720–7729.
(25) Vimr, E. R.; McCoy, R. D.; Vollger, H. F.; Wilkison, N. C.; Troy, F. A. *Proc. Natl. Acad. Sci. U.S.A.* **1984**, *81*, 1971–1975.
(26) Livingston, B. D.; McCoy, R. D.; Jacobs, J. L.; Glick, M. C.; Troy, F. A. *J. Biol. Chem.* **1988**, 9443–9448.
(27) Seidenfaden, R.; Krauter, A.; Schertzinger, F.; Gerardy-Schahn, R.; Hildebrandt, H. *Mol. Cell. Biol.* **2003**, 5908–5918.
(28) Dall'Olio, F.; Chiricolo, M. *Glycoconjugate J.* **2001**, *18*, 841–850.
(29) Ledermann, J. A.; Pasini, F.; Olabiran, Y.; Pelosi, G. *Int. J. Cancer* **1994**, *8*, 49–52.
(30) Theodosis, D. T.; Bonhomme, R.; Vitiello, S.; Rougon, G.; Poulain, D. A. *J. Neurosci.* **1999**, *19*, 10228–10236.
(31) Rutishauser, U. *J. Cell. Biochem.* **1998**, 304–312.
(32) Storms, S. D.; Rutishauser, U. *J. Biol. Chem.* **1998**, 27124–27129.
(33) Bruses, J. L.; Rutishauser, U. *J. Cell Biol.* **1998**, *140*, 1177–1186.
(34) Seki, T.; Rutishauser, U. *J. Neurosci.* **1998**, *18*, 3757–3766.
(35) Risseeuw, M. D. P.; Overhand, M.; Fleet, G. W. J.; Simone, M. I. *Tetrahedron: Asymmetry* **2007**, *18*, 2001–2010.
(36) Schweizer, F. *Angew. Chem., Int. Ed.* **2001**, *41*, 230–253.
(37) Gruner, S. A. W.; Locardi, E.; Lohof, E.; Kessler, H. *Chem. Rev.* **2002**, *102*, 491–514.
(38) Chandrasekhar, S.; Reddy, M. S.; Jagadeesh, B.; Prabhakar, A.; Ramana Rao, M. H. V.; Jagannadh, B. *J. Am. Chem. Soc.* **2004**, *126*, 13586–13587.
(39) Brisson, J. R.; Baumann, H.; Imberty, A.; Perez, S.; Jennings, H. J. *Biochemistry* **1992**, *31*, 4996–5004.
(40) Yamasaki, R.; Bacon, B. *Biochemistry* **1991**, *30*, 851–857.
(41) Szabo, L.; Smith, B. L.; McReynolds, K. D.; Parrill, A. L.; Morris, E. R.; Gervay, J. *J. Org. Chem.* **1998**, *63*, 1074–1078.
(42) Gregar, T. Q.; Gervay-Hague, J. *J. Org. Chem.* **2004**, *69*, 1001–1009.

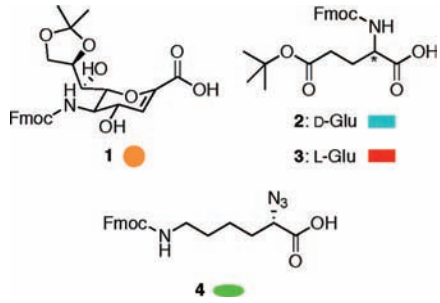

Figure 2. Amino acids used for constructing the α/δ hybrid peptides.

α-(2,8)-linked Neu5Ac helices, which require a minimum of six residues for helicity and 10 residues for stable secondary structure.[39] Because of spectral overlap and the fact that properly parametrized computational programs were not accessible, we were not able to solve the solution-phase structures of the amide-linked homo-oligomers using NMR. Also, because crystal structures have not been forthcoming, direct structural comparisons between amide- and glycosidically linked oligomers have not been possible until now.

In an effort to address the problem of spectral overlap, we designed a series of heterooligomers composed of glutamic acid and a SAA analogue of sialic acid known as Neu2en (Figure 2, **1**). Neu2en was chosen as the SAA because earlier studies from our laboratory indicated that homo-oligomers composed of this building block were the most stable and synthetically accessible.[42] Glutamic acid was chosen on the basis of its anionic charge at biological pH, which could serve as a surrogate for the carboxylates present in polymeric α-(2,8)-linked Neu5Ac. We reasoned that while the backbone structures of glycosidically and amide-linked sialic acids may not be similar, perhaps the helices could be aligned on the basis of charge distribution.

Results

Only a few synthetic hybrid peptides that assume helices have been reported.[14,43−45] In a particularly nice example reported by Gellman and co-workers, matched α/β pairs constructed from L-α-residues (Ala, Glu, Lys, Tyr), (*S*,*S*)-*trans*-2-aminocyclopentanecaboxylic acid, and (3*R*,4*S*)-*trans*-aminopyrrolidine-4-carboxylic acid were shown to adopt helical conformations in MeOH.[46] Inspired by these findings, we designed four series of tetrameric and hexameric constructs made of alternating amino acid residues having either **1**, **2**, or **3** at the N-terminus (Figure 3). Fmoc−Neu2en **1** was synthesized following our previous method[42] with slight modification to give an overall yield of 32% in eight steps (Supporting Information). Rink amide resin and BOP were used as solid support and coupling agent for SPPS, respectively, because we have previously established these to be optimal reagents.[41,42] Fmoc-α-azido-ε-aminocaproic acid linker (N_3Lys) **4** was prepared from Boc−Lys(Fmoc)−OH by Cu(II)-catalyzed NH_2 to N_3 interconversion at 92% yield.[47]

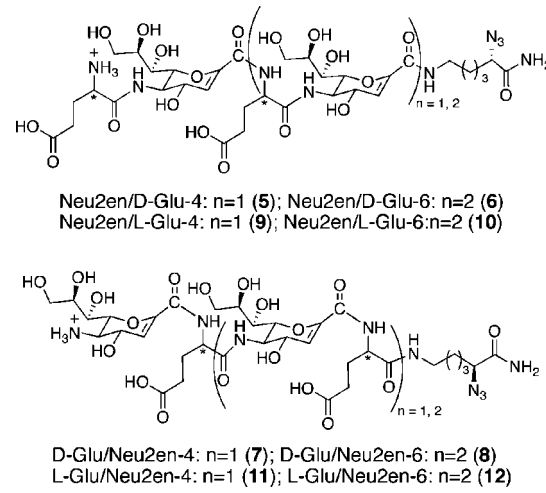

Figure 3. Synthetic design of α/δ peptides derived from **1** and **2** or **3**.

Oligomerization utilized Fmoc chemistry and commenced with coupling of **4** to the resin to prevent fraying of the C-terminus as well as to introduce the azide as a handle for future functionalization of the scaffold. In contrast to our previous SPPS of Neu5Ac oligomers that takes several hours for each coupling and deprotection step,[42] we employed microwave technology to effect shorter coupling (5 min) and deprotection (3 min) times. The use of microwave energy is believed to prevent the growing peptide chain from aggregating,[48] and this method has been successfully employed in the generation of a library of helical β-peptides.[49] Fmoc was removed using 6% piperazine, and iterative coupling and deprotection were implemented to build the oligomers according to the synthetic design. The peptides were cleaved with 30% TFA/CH_2Cl_2, concentrated in vacuo, and purified by RP-C_{18} HPLC to furnish 22−39% overall yields of α/δ hybrid foldamers.

IR Monitoring of SPPS. On the basis of our previous experience, we found that the Kaiser test[50] can be ambiguous as a basis for monitoring the deprotection of **1** on bead. We opted to use IR spectroscopy to monitor the completion of each coupling and deprotection step by recording the spectrum of the bead and bound oligomers using attenuated total reflectance (ATR) techniques. Although several studies have been published using on-bead IR monitoring,[51,52] we have discovered further use of our IR data. We found that we could use the distinct broad, strong IR absorption band at 1719 cm^{-1} due to the carbamate C═O of Fmoc as a useful marker for the extent of coupling and deprotection (Supporting Information). In addition, we could quantify the number of residues incorporated using the azide absorption at 2101 cm^{-1} as an internal standard. There is a linear correlation in the ratio of peak area integrations of azide versus amide as shown for **6** (Supporting Information). By plotting the azide/amide peak area integration of an oligomer bound to the bead and comparing it to the plot from one of our

(43) De Pol, S.; Zorn, C.; Klein, C. D.; Zerbe, O.; Reiser, O. *Angew. Chem., Int. Ed.* **2004**, *43*, 511–514.
(44) Sharma, G. V. M.; Nagendar, P.; Jayaprakash, P.; Krishna, P. R.; Ramakrishna, K. V. S.; Kunwar, A. C. *Angew. Chem., Int. Ed.* **2005**, *44*, 5878–5882.
(45) Schmitt, M. A.; Choi, S. H.; Guzei, I. A.; Gellman, S. H. *J. Am. Chem. Soc.* **2006**, *128*, 4538–4539.
(46) Hayen, A.; Schmitt, M. A.; Ngassa, F. N.; Thomasson, K. A.; Gellman, S. H. *Angew. Chem., Int. Ed.* **2004**, *43*, 505–510.
(47) Nyffeler, P. T.; Liang, C.-H.; Koeller, K. M.; Wong, C.-H. *J. Am. Chem. Soc.* **2002**, *124*, 10773–10778.
(48) Collins, J. M.; Leadbeater, N. E. *Org. Biomol. Chem.* **2007**, *5*, 1141–1150.
(49) Murray, J. K.; Farooqi, B.; Sadowsky, J. D.; Scalf, M.; Freund, W. A.; Smith, L. M.; Chen, J.; Gellman, S. H. *J. Am. Chem. Soc.* **2005**, *127*, 13271–13280.
(50) Kaiser, E.; Colescat, R. L.; Bossinge, C. D.; Cook, P. I. *Anal. Biochem.* **1970**, *34*, 595.
(51) Yan, B. *Acc. Chem. Res.* **1998**, *31*, 621–630.
(52) Huber, W.; Bubendorf, A.; Grieder, A.; Obrecht, D. *Anal. Chim. Acta* **1999**, *393*, 213–221.

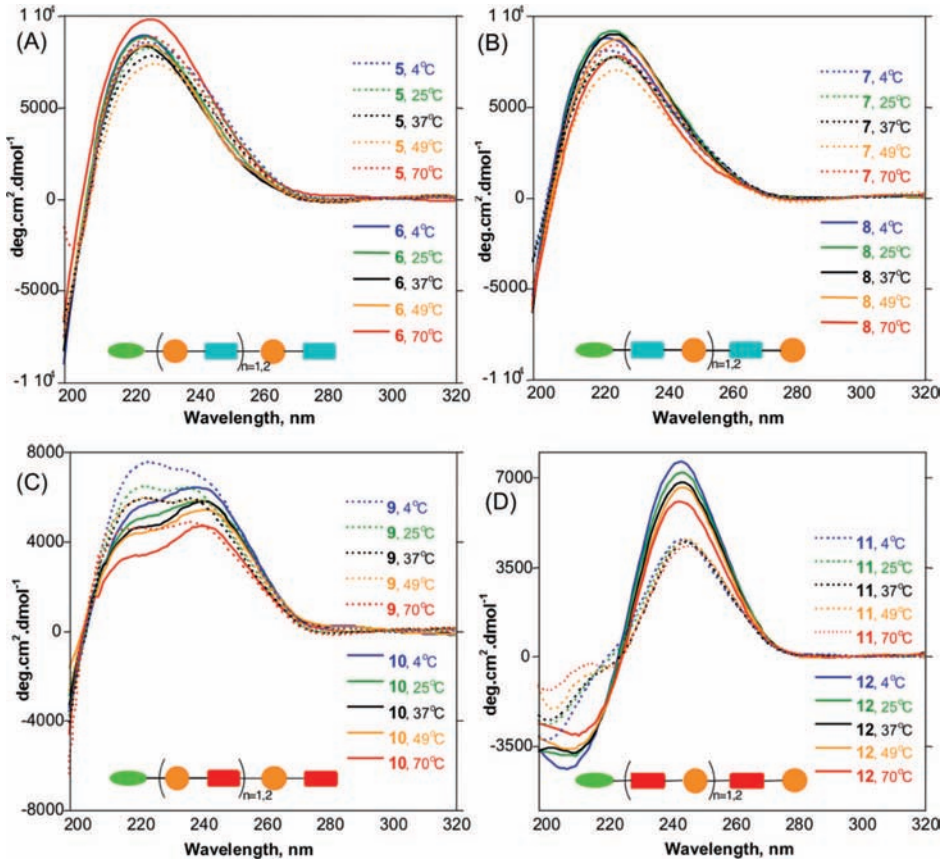

Figure 4. CD spectra of α/δ peptides in PBS, pH 7.4, at different temperatures normalized per residue. (A and B) Spectra of **5**−**8** showing positive CD bands at 223 nm indicating random coils. (C) Spectra of **9** and **10** showing an unusual double positive Cotton effect due to an unstable 2° structure. (D) Spectra of **11** and **12** showing a unique spectral signature distinct from a typical amide band. Peak to trough analysis indicates increasing stability of 2° structure from tetramer to hexamer.

trials, we determined the number of residues of a bead-bound heterooligomer of known peptide sequence without going through a more tedious analytical process like mass spectrometry, which typically requires cleavage from the bead.

Conformational Studies by CD. We probed the 2° structure of the α/δ hybrid peptides in PBS buffer by CD at pH 7.4 to mimic physiological conditions. Spectra were recorded at various temperatures from 4 to 70 °C. Molar ellipticities were divided by the number of **1** and Glu residues to normalize the contribution of each residue to the secondary structure of the oligomer, because the additivity of the residues is not linear and is dependent on the stability of the conformation assumed by the peptide.[41] CD has been used to characterize solution-phase 2° structures of peptides,[53,54] and good correlation with crystal structure has been observed.[55] We have also demonstrated by CD that unnatural amide-linked analogues of sialic acid form stable 2° structures in water.[41,56]

The CD profiles of **5**−**8** in Figure 4A and B show a positive Cotton effect centered at 223 nm of the amide region. Within these series, no significant differences in [θ]'s were observed by varying the length or temperature. This is reminiscent of unfolded α-peptides that have random behavior.[57] The conjugated amide chromophore of **1** in **5**−**8** did not show a π to π^* transition at longer wavelength, which further suggests that these compounds do not assume any stable conformation and are random coils in aqueous medium. Compounds **9** and **10** show unusual double positive Cotton effects that look as if the trough at 220 nm is flipped horizontally (Figure 4C). The intensity of the peak at 220 nm decreases with increasing length, suggesting that interconversion between random and 2° structure may be occurring. We considered that this CD profile may be the average of the dynamic folding and unfolding behavior of **9** and **10** in aqueous solution and may be indicative of weak H-bonds that are easily disrupted by water.

Figure 4D shows the CD spectra of **11** and **12** exhibiting Cotton effects at 202 and 245 nm for **11** and 209 and 243 nm for **12**. These profiles are different from those previously observed for helical α-, β-, or γ-peptides. The $\pi \rightarrow \pi^*$ transition of the conjugated olefinic double bond of **1** displays a unique longer wavelength spectral signature. The intensity of these bands is dependent on oligomer length and temperature. Peak to trough analysis reveals increasing stability with length, and decreased peak intensity at higher temperatures (Table 1), the hexamer **12** being more stable than the tetramer **11**. We

(53) Nicoll, A. J.; Weston, C. J.; Cureton, C.; Ludwig, C.; Dancea, F.; Spencer, N.; Smart, O. S.; Gunther, U. L.; Allemann, R. K. *Org. Biomol. Chem.* **2005**, *3*, 4310–4315.
(54) Kawamura, S. I.; Morita, T.; Kimura, S. *Sci. Technol. Adv. Mater.* **2006**, *7*, 544–551.
(55) Appella, D. H.; Christianson, L. A.; Klein, D. A.; Powell, D. R.; Huang, X. L.; Barchi, J. J.; Gellman, S. H. *Nature* **1997**, *387*, 381–384.
(56) McReynolds, K. D.; Gervay-Hague, J. *Tetrahedron: Asymmetry* **2000**, *11*, 337–362.
(57) Woody, R. E. In *Circular Dichroism and the Conformational Analysis of Biomolecules*; Fasman, G. D., Ed.; Plenum Press: New York, 1996; pp 25−67.

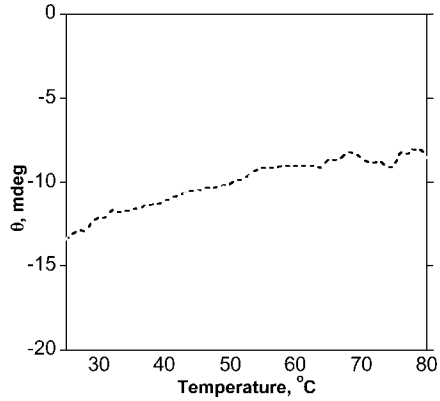

Figure 5. Variable-temperature CD of **12** for the Cotton effect at 209 nm. No sharp inflection point was observed, indicating no cooperative breakup of H-bonds.

Table 1. Analyses of Peak and Trough of Molar Ellipticities of **11** and **12** Indicate Increase in 2° Structure Stability with Length and Decrease at Higher Temperatures

	L-Glu/Neu2en-4 (**11**)			L-Glu-Neu2en-6 (**12**)		
temp (°C)	peak max	peak min	peak−trough	peak max	peak min	peak−trough
4	4578.8	−3244.0	7822.8	7596.4	−4379.7	11 976.1
25	4460.7	−2694.0	7154.7	7167.3	−3881.3	11 048.6
37	4425.4	−2536.7	6962.1	6749.0	−3845.7	10 594.7
49	4548.5	−2093.1	6641.6	6538.2	−3687.3	10 225.5
70	4301.1	−1334.0	5635.1	5982.5	−3100.7	9083.2

interpreted these CD profiles to indicate that these constructs are matched and form ordered 2° structures in water.

Thermal Stability. Typical CD patterns of proteins that possess stable 2° structures often show a sharp inflection point upon heating due to denaturation.[58] We recorded the temperature-dependent CD spectrum of **12** to probe if its conformation is stabilized by cooperative folding processes due to stabilization by H-bonds between the amide NH and carbonyl oxygen of the backbone. Figure 5 shows a steady decrease in intensity for the Cotton effect at 209 nm that remains almost linear upon heating to 80 °C, reflecting no breakup in the 2° structure. This noncooperative mechanism has been observed in thermally stable α-helical peptides,[59] as well as in helical β-peptides stabilized by staggering effects.[60] We hypothesized that this noncooperative behavior could be due to strong intramolecular H-bonding that stabilizes the secondary structure of **12**.

NH/ND Exchange. It has been demonstrated that slow NH/ND exchange rates are indicative of stable 2° structure in oligopeptides.[5,41] We noticed during our initial ^{1}H NMR studies that the H/D exchange of amide H in D_2O is instantaneous at room temperature. Therefore, we opted to perform the NH/ND exchange study in D_2O at 277 K to slow the exchange at a rate that is observable on the NMR time scale. Spectra of **6**, **8**, **10**, and **12** were recorded over time, the integration of the amide peaks were measured at each time point, and the half-life ($t_{1/2}$) of NH/ND exchange was calculated based upon pseudo first-order kinetics. The C-terminal amide hydrogens were completely exchanged prior to the acquisition of the first FID. This rapid exchange suggests that in aqueous solutions, the C-termini of these peptides are fully exposed to the solvent and do not form intramolecular H-bond. The internal amide NH resonances of **6**, **8**, and **10** showed a large difference in exchange rates as compared to **12** as a function of sequence and Glu configuration. Figure 6 shows the long $t_{1/2}$ of the amide H of **12** at 17−86 min, suggesting a 2° structure stabilized by intramolecular H-bond. The amide H's of **6** and **8** have relatively short $t_{1/2}$ values of 3−8 min, while those of **10** have a $t_{1/2}$ of 5 min that is equivalent to about 3−6 times the exchange rate of **12** that suggest unfolded peptide chains. We also performed the NH/ND exchange study in DMSO-d_6 solution at 298 K with the addition 10% D_2O (Supporting Information) and observed consistent fast relative deuterium exchange rates of **6** and **8** to **12**, while **10** showed twice the exchange rate of **12**. Figure 7 includes a stack plot of ^{1}H NMR spectra of **12** in (a) D_2O and (b) DMSO-d_6 + D_2O recorded at different time points, showing the differential deuterium exchange of amide protons. Noteworthy is the fact that in DMSO-d_6, a significant amount of NH amides of Glu4 (10%), Glu6 (9%), and N_3Lys (14%) in **12** remains unexchanged after 20 h. This relatively slow exchange suggests a strong intraresidue H-bonding that is responsible for the stable 2° structure of **12**. We also observed that NH amides of **12** are more dispersed and distinct from each other as compared to **6**, **8**, and **10** (Supporting Information). These findings strongly corroborate our CD observations, indicating the stable 2° of **12**.

Conformational Studies by NMR. Detailed ^{1}H and 2-D homonuclear ROESY NMR studies were performed on **8**, **10**, and **12** in 9:1 H_2O/D_2O to elucidate their structures in solution. Although the kinetics and CD profiles of **8** indicate a random coil, this oligomer was included in the NMR conformational analysis to demonstrate the impact of amino acid configuration on 2° structure stability, while **10** was chosen to probe sequence specificity. Figure 8 is a stack plot of the amide region of the ^{1}H NMR spectra for **8**, **10**, and **12** and demonstrates the sequence and configuration dependence of their 2° structures. The greater chemical shift dispersion of Glu amide resonances of **12** suggests the presence of 2° structure. This observation is in agreement with our findings in CD spectroscopy. The wider dispersion of amide ^{1}H chemical shifts for **12** is in contrast to overlapping amide resonance peaks found in **8** and **10**, suggesting that **8** and **10** lack ordered structure, which is in agreement with their random coil conformation observed by CD.

ROESY spectra were recorded for **8**, **10**, and **12** to analyze their three-dimensional main chain conformations. Initial ^{1}H NMR studies were performed on the tetramers to differentiate terminal and internal residues and facilitate the assignment of resonances for the hexamers (Supporting Information). A preliminary ROESY experiment was performed on L-Glu/Neu2en dimer to differentiate between intra- and inter-residue NOE of Neu2en. ROESY cross peaks were calibrated into distance restraints for solution-phase structure calculations using restrained molecular dynamics and simulated annealing in XPLOR-NIH.[61] The effect of solvent and solvent screening of electrostatic charges in the X-PLOR structure calculation was implemented using the 1/R dielectric option for the electrostatic energy function in XPLOR (Supporting Information). The parameter and topology files for Neu2en and N_3Lys were generated by modifying previously known data for Neu5Ac and

(58) Benjwal, S.; Verma, S.; Rohm, K. H.; Gursky, O. *Protein Sci.* **2006**, *15*, 635–639.
(59) Patgiri, A.; Jochim, A. L.; Arora, P. S. *Acc. Chem. Res.* **2008**, *41*, 1289–1300.
(60) Gademann, K.; Jaun, B.; Seebach, D.; Perozzo, R.; Scapozza, L.; Folkers, G. *Helv. Chim. Acta* **1999**, *82*, 1–11.
(61) Schwieters, C. D.; Kuszewski, J. J.; Tjandra, N.; Clore, G. M. *J. Magn. Reson.* **2003**, *160*, 65–73.

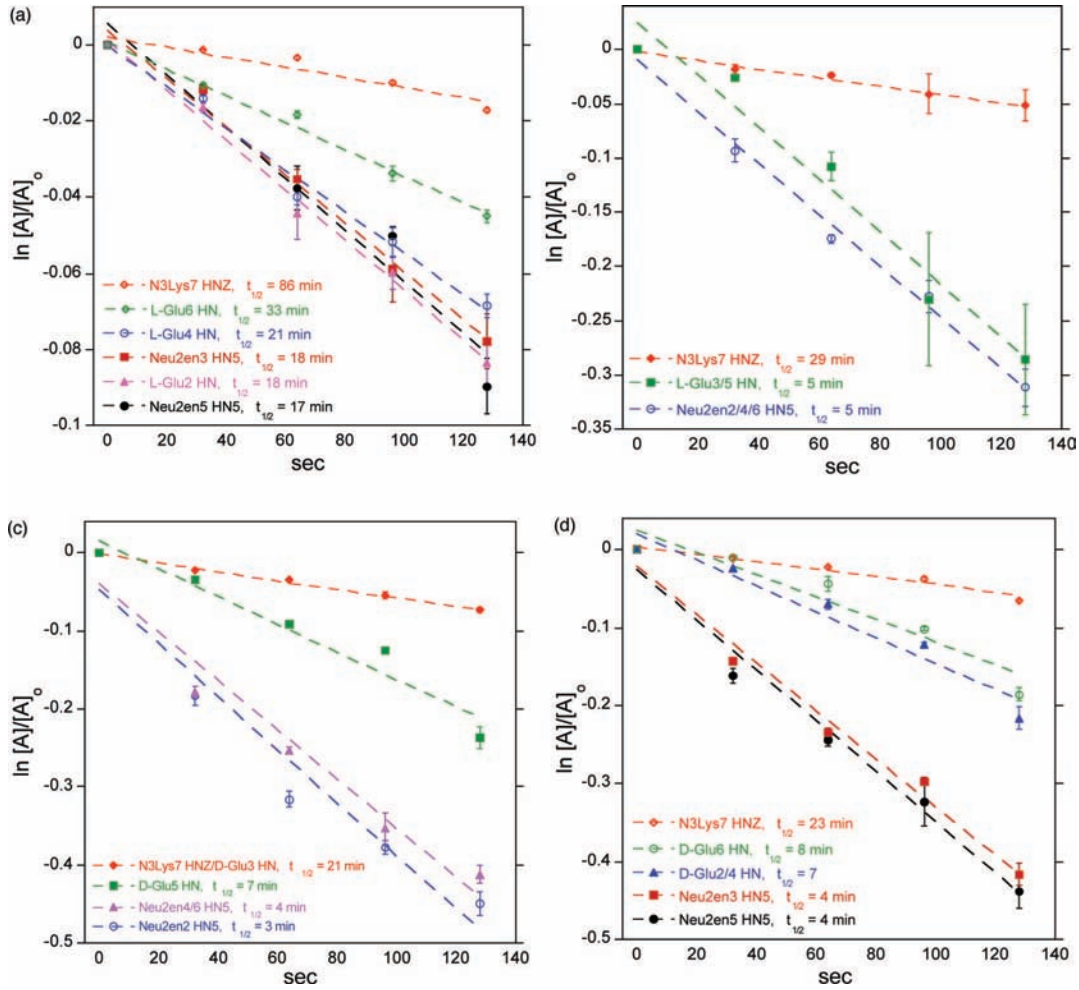

Figure 6. Pseudo first-order rate plots showing the long $t_{1/2}$ of H-bonded amide protons of **12** (a) indicating a 2° structure stabilized by intramolecular amide H-bonds. The amide H's of **6** (c) and **8** (d) have relatively shorter $t_{1/2}$ of 3−8 min, while those of **10** (b) have $t_{1/2}$ of 5 min that is equivalent to about 3−6 times the NH/ND exchange rate of **12**, suggesting unfolded peptide chain.

L-Lys, and the azide parameters were obtained from previously reported ab initio calculations.[62] The phi and psi dihedral restraints for L-Glu NH were estimated from the chemical shift index[63] and from empirical values of $^3J_{HN,H\alpha}$.[64] The lowest energy structures without NOE violations were selected, averaged, and energy minimized.

A number of ROESY cross peaks for **12** were assigned that help define its overall main chain conformation. In particular, the most prominent long-range ROESY cross peaks include the recurring Neu2en-H8(i)→L-Glu-HN(i+1), Neu2en-H3(i)→Neu2en-H9′(i+2), L-Glu2-Hα→L-Glu4-HN, and N_3Lys7-H2→L-Glu4-Hγ (Figure 9). The secondary structure of **12** in water is defined by 76 NOE restraints deduced from the ROESY experiment.

A total of 25 low energy structures were selected, and a side view of a bundle of seven is shown in Figure 10A. The backbone rmsd of 0.699 Å and a rmsd of 1.422 Å for all non-H atoms indicate good convergence of the calculated structures (Table 2). Figure 10B is the side view of the averaged, minimized structure of **12**. There are three recurring H-bonds between L-Glu HN and Neu2en pyranose ring oxygen having the same bond lengths of 2.4 Å. This interaction appears to be unique to sialic acid, and, to our knowledge, this H-bond pattern has not been reported in previous SAA studies. A classical C═O···H−N at 2.6 Å was also found at the center of the peptide chain between Neu2en-3 and Neu2en-5, which significantly contributed to the stability of **12**. Although it was previously reported that "nearest-neighbor" five- or seven-membered ring H-bonds are unfavorable for α and 3_{10} helices of proteins,[1] our novel α/δ hybrid peptides do not obey this behavior and form a seven-membered ring. Furthermore, there is a direct correlation between these H-bonds and the slow NH/ND exchange rates that we observed for **12** in the kinetic studies.

The top view of **12** from the N-terminus (Figure 10C) shows that the upfield C-terminal NH_2 of N_3Lys, observed as singlets at 7.25 and 7.64 ppm in DMSO-d_6 (Supporting Information), are solvent exposed, which accounts for their fast deuterium exchange, while the azide is oriented outward making it accessible for future functionalization with relevant small molecule ligands using 1,2-dipolar cycloaddition. The Glu side chain carboxylates are fully solvated, and each succeeding Glu residue is oriented opposite from the previous one, separated

(62) Sklenak, S.; Gatial, A.; Biskupic, S. *J. Mol. Struct. (THEOCHEM)* **1997**, *397*, 249–262.
(63) Wishart, D. S.; Sykes, B. D.; Richards, F. M. *Biochemistry* **1992**, *31*, 1647–1651.
(64) Kuboniwa, H.; Grzesiek, S.; Delaglio, F.; Bax, A. *J. Biomol. NMR* **1994**, *4*, 871–878.

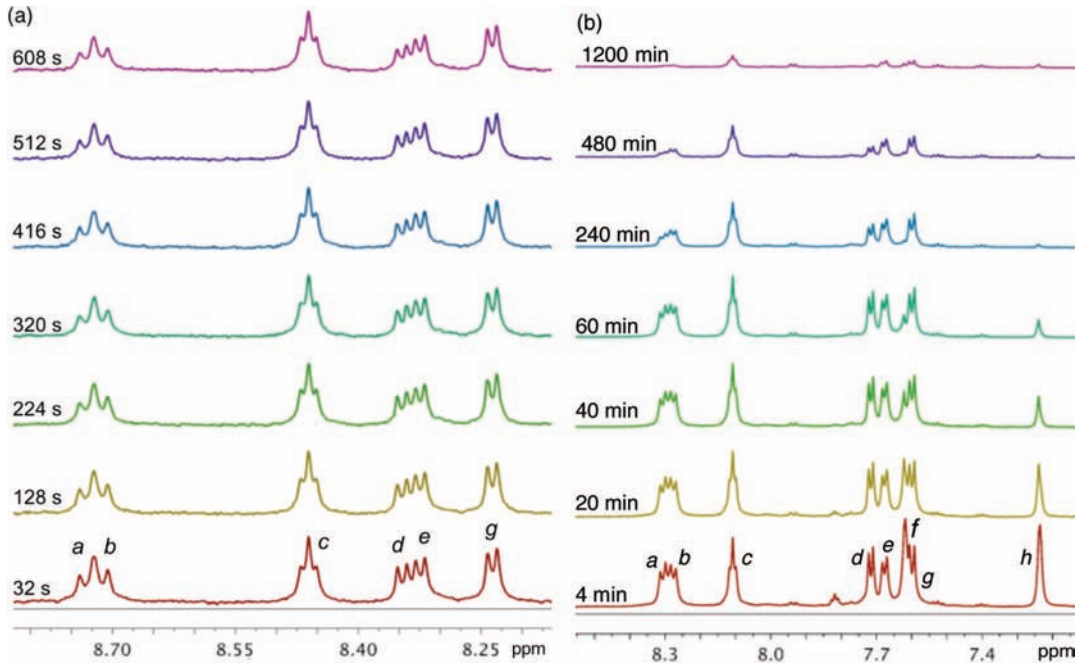

Figure 7. Stack plot of ^{1}H NMR spectra of **12** in (a) D_2O, 277 K and (b) DMSO-d_6, 298 K at different times after addition of D_2O, 600 MHz. a and b, HN5 of Neu2en3 and 5; c, f, and h, HNZ, H2, and H1 of N_3Lys7, respectively; d, e, and f, HN of L-Glu2, 4, and 6, respectively.

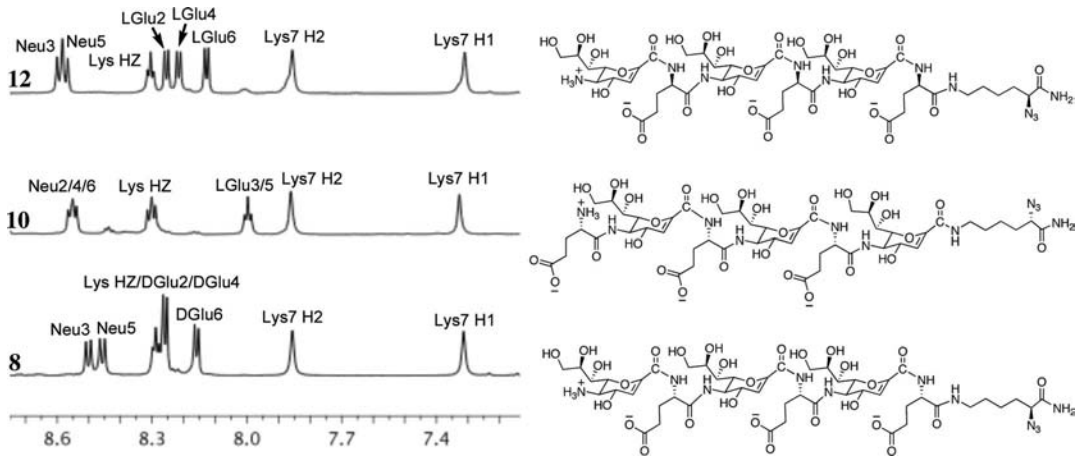

Figure 8. Stack plot of the amide regions from the ^{1}H NMR spectra of **8**, **10**, and **12** in 9:1 H_2O/D_2O, 600 MHz, 298 K (Neu = Neu2en; Glu = glutamic acid; Lys = N_3Lys).

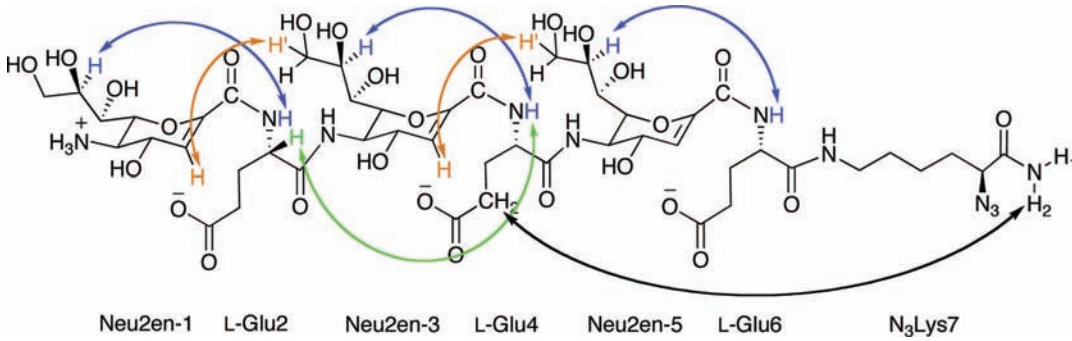

Figure 9. Crucial long-range NOE's for **12** extracted from the ROESY spectra (9:1 H_2O/D_2O). Neu2en-H8(i)→L-Glu HN(i+1) NOE's are in blue, Neu2en-H3(i)→Neu2en-H9′(i+2) are in brown, L-Glu2-Hα→ L-Glu4-HN is in green, and N_3Lys7-H2→L-Glu4-Hγ is in black.

by an average distance of 14.1 Å, while Glu2 and Glu6 carboxylates are 11.8 Å apart. This satisfies the electrostatic stabilization due to maximum separation of negative charges, which is consistent with a model for αNeu5Ac(2→8)αNeu5Ac octamer calculated using complete relaxation matrix analysis.[40]

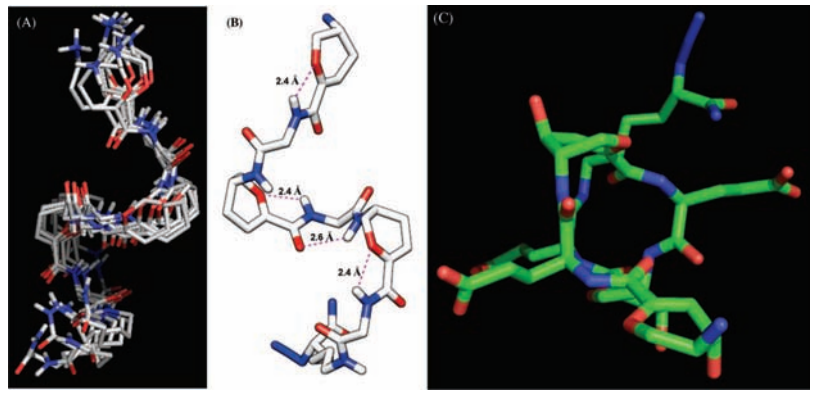

Figure 10. (A) A bundle of selected seven low-energy NMR derived structures of foldamer **12** calculated using XPLOR-NIH using NOE restraints generated from ROESY spectra in 9:1 H_2O/D_2O at 500 ms mixing time, 600 MHz, 298 K. (B) Side view of the averaged and minimized solution-phase NMR structure of **12** showing the intraresidue ring O→H−N and C═O→H−N bonds. (C) Top view from the N-terminus showing fully extended and solvated Glu side chains (all H have been omitted for clarity).

Table 2. Properties of 25 Lowest Energy Calculated Structures of **10** and **12**

	Neu2en/ L-Glu-6 (**10**)	L-Glu/ Neu2en-6 (**12**)
rmsd for Neu2en and L-Glu backbone, Å	0.867 ± 0.384	0.699 ± 0.220
rmsd for non-H atoms, including side chains, Å	1.520 ± 0.375	1.422 ± 0.280
inter-residue amide H bonds	3	4
total number of NOEs	82	76
final energy, kcal/mol	352.289	354.169

The NMR solution-phase structure of **10** was studied using the same approach above for **12**. Figure 11 is the minimized average structure with a backbone rmsd of 0.867 ± 0.384 and rmsd of 1.520 ± 0.375 for non-H atoms. This structure clearly shows a lack of defined helical pattern as well as less ordered arrangement of L-Glu side chains. A total of three H-bonds were found between L-Glu3, L-Glu5 HN, and N_3Lys7 epsilon HN and pyranose ring *O*. Oligomer **10** lacks the classical backbone H-bond found in **12**, which demonstrates the significance of sequence specificity for establishing a stable 2° structure.

Fewer H-bonds account for the instability of **10**, suggesting that it interconverts between random and folded structures, which is in agreement with the CD and kinetics studies. The NMR solution-phase structure of **8** was also analyzed, but did not yield defined conformations: the low energy structures do not converge to a single, preferred conformation. However, an overlay of 25 low energy structures showed extended, random coils (Supporting Information), which is in agreement with the CD and kinetics data. No further conformational analysis was undertaken for **8**. The instability of the conformation of **10** and the absence of a defined structure in **8** clearly indicate that the 2° structure of Neu2en/Glu peptides is defined by the appropriate peptide sequence and the configuration of L-Glu that is found in both **11** and **12**. The results suggest that all L-α-amino acids will have the matched configuration with Neu2en, which paves the way for the design and construction of neutral, cationic, or zwitterionic Neu5Ac-based foldamers.

Comparisons of α-(2→8)Neu5Ac Polymer and Neu2en/L-Glu Foldamer Conformations. Conformational studies of α-(2→8)Neu5Ac polymer indicate that it exists primarily as a random coil with localized regions of helicity. A human monoclonal macroglobulin IgM^{NOV} with specificity for α-(2,8)-linked Neu5Ac polymer has been identified.[65] This antibody also shows cross-reactivity with polynucleotides and denatured DNA, which bind to the same site that recognizes α-(2,8)-linked Neu5Ac polymer.[65] NMR investigations of the helical regions of α(2→8)Neu5Ac polymer resulted in the identification of three major conformers differing in the number of residues per turn (*n*) and the chirality of the helix. The $G1^+$ and $G3^+$ conformers are right-handed helices of $n = 2$ and 9, respectively, while $G2^+$ is left handed with $n = 4$.[39] Comparisons between the $G3^+$ helical epitope and the structure of poly (A) nucleotide showed remarkable similarities, most notably in the positioning of the charged functional groups.[39] This finding led to the hypothesis that antibody cross-reactivity arises from the appropriate spatial arrangement of negative charge.[65] On the basis of this hypothesis, we have explored the possibility of creating stable Neu2en/Glu foldamers that can serve as novel scaffolds for carboxylate display. To that end, comparisons of **12** with the predicted conformations of α-(2,8)-linked Neu5Ac polymer indicate that the carboxylate periodicity of **12** closely maps to the $G2^+$ helix with one-half the charge density (Figure 12). However, the $G2^+$ helix is left-handed, whereas **12** is right-handed. Furthermore, the *n* of **12** is much smaller than the extended helical antigenic $G3^+$ conformer of poly-α(2→8)Neu5Ac, leading to the prediction that **12** would not be cross-reactive with IgM^{NOV} based on this conformational difference.[39]

Conclusions

We have constructed a novel class of functionalizable Neu5Ac-derived, water-soluble α/δ hybrid peptides using microwave-assisted SPPS. Constructs made from **1** and **3** (**11**, **12**) are matched and form stable 2° structures in aqueous solution, while those from **1** and **2** (**5**−**8**) are mismatched and are random coils. We have shown here that stable 2° structure is affected by both the configuration of Glu and the peptide sequence. Our findings indicate that **12** is not only stabilized by traditional C═O···H−N backbone H-bonding but by a net effect of factors that include the following: (a) inherent rigidity of the flattened pyranose ring and the conjugated amide linkage, (b) appropriate configuration and position of Glu in the peptide sequence, (c) H-bond between L-Glu HN and Neu2en ring *O*, and (d) minimized electrostatic repulsion between the L-Glu side chains. Because the synthesis of these peptides is modular, we

(65) Kabat, E. A.; Liao, J.; Osserman, E. F.; Gamian, A.; Michon, F.; Jennings, H. J. *J. Exp. Med.* **1988**, *168*, 699–711.

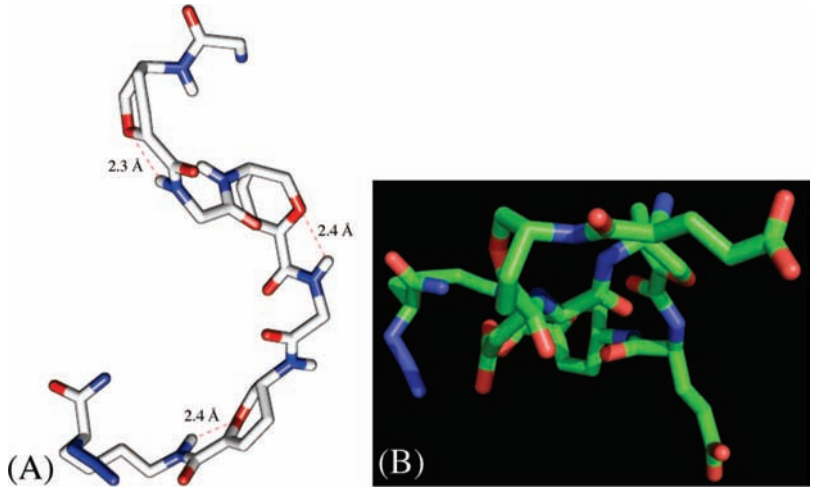

Figure 11. Minimized average structure of **10** showing a lack of defined helical pattern as well as less ordered arrangement of L-Glu side chains (OH and aliphatic H have been omitted for clarity): (A) side view; (B) top view.

can tailor the length, as well as the charge, by replacing Glu to match the size and charge of the intended target. We anticipate that the design process will be greatly facilitated now that we have access to appropriately parametrized computational programs that can be used to predict the conformations of modified structures.

This Article has focused on establishing fundamental principles for scaffold design with the long-term objective of making immunogenic surrogates of α(2→8)Neu5Ac polymer. One target antibody, IgM^{NOV}, recognizes the $G3^+$ conformational epitope of α-(2,8)-linked Neu5Ac polymer. However, given the conformational flexibility of the Neu5Ac polymer, it is conceivable that antibodies against alternative conformations of α(2→8)-Neu5Ac polymer (e.g., $G1^+$ or $G2^+$) could be elicited upon exposure to antigenic epitopes. There are difficulties associated with using α-(2,8)-linked Neu5Ac polymer to elicit antibody production because the polymer is susceptible to enzymatic degradation by neuraminidase and it is poorly immunogenic due to its role in human embryonic development. An alternative approach to producing antibodies against conformational epitopes of α-(2,8)-linked Neu5Ac would be to develop enzymatically stable foldamers such as **12** that may be capable of eliciting a cross-reactive antibody response. The studies outlined in this Article establish a viable platform for synthesizing and designing foldamers with this intended purpose. Our future plans include studies to determine the plasma stability of these foldamers as well as their immunogenic properties.

Experimental Section

Experimental procedures for the synthesis of **1** and **4** are fully described in the Supporting Information.

Solid-Phase Synthesis of α/*δ* Hybrid Peptides. Typically, 100 mg of Fmoc−Rink resin (0.5 mmol/g) was swelled in DMF for 2 h and drained. Every coupling and Fmoc deprotection step was monitored by IR spectroscopy as described below. Fmoc deprotection required 6% piperazine in NMP using an open polypropylene tube with fritted disk and microwave irradiation in a microwave reactor equipped with a fiber optic temperature sensor. Reaction conditions were as follows: power = 30 W, ramp time = 1 min, hold time = 3 min, temperature = 75 °C. The resin was washed with MeOH (2 mL × 3) and CH_2Cl_2 (2 mL × 3). N_3Lys (**4**) (86.4 mg, 2 equiv), BOP (97 mg, 2 equiv), DIPEA (57 mg, 4 equiv), and 2 mL of NMP were added to the resin and mixed and allowed to sit at room temperature for 10 min. Microwave coupling conditions are the same as in the deprotection, except for the 5 min hold time, and the loading process was repeated using 1 equiv of **4**, 1 equiv of BOP, and 4 equiv of DIPEA to ensure complete loading. The succeeding coupling reactions were performed using **3** or **1**, followed by iterative deprotection and coupling steps between incorporation of amino acid. The oligomer was cleaved from the resin with 30% TFA in CH_2Cl_2 (5 mL × 30 min agitation × 5), and the filtrates were pooled, concentrated in vacuo, diluted in 5 mL of H_2O, and lyophilized. This process also hydrolyzed the isopropylidene of **1** as well as the *t*-butyl ester of Glu. The crude peptide was purified by reverse phase HPLC (RP-C_{18}, 10 × 250 mm; 5−50% aqueous MeOH with 0.1% TFA) with detection set at 225 and 260 nm. Eluates were concentrated and lyophilized to yield white, fluffy solid TFA salt of the peptide.

L-Glu/Neu2en-6 (12). This was obtained in 22% purified yield. ^{1}H NMR (D_2O, 600 MHz): d 5.97 (d, 1H, *J* = 3.0 Hz, H3−1), 5.92 (d, 2H, *J* = 2.4 Hz, H3−3/5), 4.68 (dd, 1H, *J* = 9.0, 3.0 Hz, H4−1), 4.65 (dd, 1H, *J* = 10.2, 1.8 Hz, H6−1), 4.57 (dd, 2H, *J* = 8.4, 2.4 Hz, H4−3/5), 4.54 (dd, 1H, *J* = 5.4, 3.6 Hz, Hα−2), 4.53 (dd, 1H, *J* = 5.4, 3.6 Hz, Hα−4), 4.45 (dd, 2H, *J* = 10.8, 1.8 Hz, H6−3/5), 4.45 (dd, 1H, *J* = 6.6, 3.6 Hz, Hα−6), 4.21 (dd, 1H, *J* = 9.6, 3.0 Hz, H5−3), 4.19 (dd, 1H, *J* = 9.0, 3.0 Hz, H5−5), 4.15 (dd, 1H, *J* = 7.8, 6.0 Hz, Hα−7), 4.09 (ddd, 1H, *J* = 9.0, 5.4, 3.0 Hz, H8−1), 4.02 (ddd, 1H, *J* = 12.6, 6.6, 2.4 Hz, H8−3), 4.01 (ddd, 1H, *J* = 12.6, 6.6, 2.4 Hz, H8−5), 3.95 (dd, 1H, *J* = 12.0, 3.0 Hz, H9′−1), 3.92 (dd, 2H, *J* = 10.8, 2.4 Hz, H9′−3/5), 3.92 (dd, 1H, *J* = 8.4, 1.8 Hz, H7−1), 3.82 (dd, 1H, *J* = 12.0, 6.0 Hz, H9−1), 3.73 (dd, 2H, *J* = 9.0, 2.4 Hz, H7−3/5), 3.72 (dd, 2H, *J* = 12.0, 6.0 Hz, H9−3/5), 3.66 (dd, 1H, *J* = 10.2, 9.0 Hz, H5−1), 3.31−3.21 (m, 2H, Hε−7), 2.59 (dd, 3H, *J* = 7.2, 7.2 Hz, Hγ′−2/4/6), 2.54 (dd, 3H, *J* = 7.2, 7.2 Hz, Hγ−2/4/6), 2.29−2.09 (m, 6H, Hβ−2/4/6), 1.91−1.79 (m, 2H, Hβ−7), 1.64−1.55 (m, 2H, Hδ−7), 1.44 (p, 2H, *J* = 7.8 Hz, Hγ−7). ^{13}C NMR (D_2O, 150 MHz): d 180.2, 180.1, 178.4, 176.5, 175.6, 166.5, 166.4, 165.9, 148.0, 112.1, 111.0, 79.2, 78.0, 72.8, 70.8, 70.6, 69.8, 67.6, 66.1, 66.0, 65.9, 65.5, 56.4, 56.3, 53.7, 52.9, 41.9, 33.8, 32.9, 30.7, 29.1, 29.0, 24.8. MALDI-TOFMS: [M + Na^+] calcd for $C_{48}H_{73}N_{11}O_{28}Na^+$, 1274.4518; found, 1274.452.

Other α/*δ*-peptides were prepared by the same method as described above, and their characterization data are found in the Supporting Information.

IR Spectroscopy. The washed resin containing the growing peptide chain was dried under suction in a manifold. Two to three beads were taken, pressed on top of the ZnSe-diamond crystal of the ATR plate, and the spectrum was recorded. The carbamate and azide absorption bands were monitored at 1719 and 2101 cm^{-1}, respectively. Absorbance peak area integration was done using a

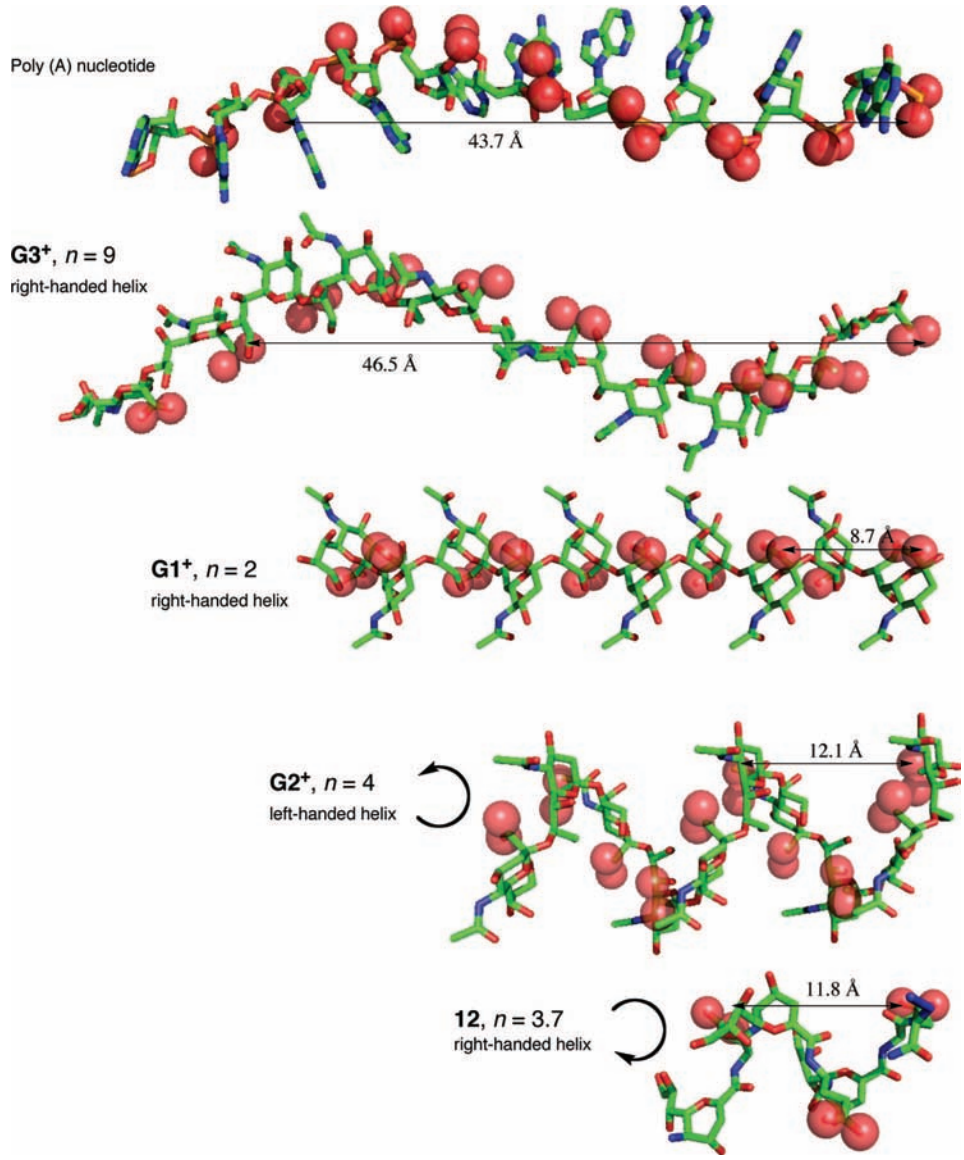

Figure 12. Comparison of **12** with the $G1^+$, $G2^+$, and $G3^+$ conformers of poly-α(2→8)Neu5Ac reveals a similar helical conformation and periodicity of carboxylate groups with one-half the charge frequency and opposite handedness of **12** to $G2^+$ (H atoms were omitted for clarity).

commercial IR software, and the ratios of amide/azide peak areas of both Fmoc-protected and deprotected peptides were plotted versus oligomer length.

Circular Dichroism. Peptides were prepared at 0.5 mg/mL in PBS, pH 7.4. Spectra were recorded in a 1 mm path length quartz cuvette with PBS as a blank at five temperatures: 4, 25, 37, 49, and 70 °C. Five scans were obtained and averaged for each sample from 320 to 198 nm with data points taken every 1.0 nm. All molar ellipticity values were normalized by dividing by the number of **1** and Glu residues in the oligomer. For the thermal stability experiment of **12**, the ellipticity at 209 nm was monitored as a function of temperature. Data were collected from 25 to 80 °C in triplicate and averaged for every 1 °C temperature increment.

Amide NH/ND Exchange. Samples were dissolved in (a) D_2O, pD 5.5 and (b) DMSO-d_6 followed by the addition of 10% D_2O by volume. ^{1}H NMR spectra were collected on a 600 MHz NMR spectrometer at 277 K, 16 scans each at 32 s interval for the D_2O solution, while the DMSO-d_6 solution was studied at 298 K, 64 scans each at 4 min interval. The pseudo first-order kinetics and half-life ($t_{1/2}$) of amide NH were calculated using the equations $\ln[A]/[A]_o = -kt$ and $t_{1/2} = \ln 2/k$, where $[A]$ is the peak area integration at time $= t$, and $[A]_o$ is the peak area integration at time $= 0$.

ROESY NMR and Solution-Phase Structure Calculations. The peptides were dissolved in 0.6 mL of H_2O/D_2O (9:1) at a concentration of 3.5−5 mM, pH 5.5. All ROESY experiments were performed at 298 K on a 600 MHz spectrometer equipped with a 5 mm cryoprobe. Water suppression was achieved by WATERGATE technique.[66] ROESY spectra were initially recorded at 50, 100, 200, 300, 400, and 500 ms mixing times, and we found 500 ms to be optimal. All data were recorded using Bruker TopSpin, and the ROESY cross-peak volumes in the contour plot were measured using MestReNova software. Restrained molecular dynamics and simulated annealing calculations were performed using the protocol of XPLOR-NIH[61] v.2.15 with initial temperature set at 1000 K with 6000 heating and 3000 cooling steps, and they incorporated the distance and dihedral angle restraints. As distance restraints, the parameters extracted from ROESY experiments were categorized into three: strong, medium, and weak with 2.9, 3.3, and 5.0 Å, respectively, as upper bond distance limits. The phi and psi dihedral angle restraints for Glu were derived from empirical data for $^3J_{HN,H\alpha}$ and chemical shift indices of α-C, α-H, and amide C and were assigned the values of −120.0 ± 30.0 and 130.0 ±

(66) Piotto, M.; Saudek, V.; Sklenar, V. *J. Biomol. NMR* **1992**, *2*, 661–665.

30.0, respectively.[63,64] Parameter and topology files for Neu2en and N_3Lys were generated by modifying previously known data for Neu5Ac and L-Lys,[61] and the azide parameters were obtained from previously reported ab initio calculations.[62] The calculations were looped to produce 100 structures, and the lowest energy structures without NOE violations were selected, averaged, and energy minimized to generate the final structure. Visualization was done using MacPyMOL[67] and UCSF Chimera.[68]

Acknowledgment. Dr. J. S. DeRopp is acknowledged for his help in WATERGATE ROESY experiments. The UC Davis NMR Award to J.G.-H. is also acknowledged. The coordinates for poly-α(2→8)Neu5Ac conformers were obtained through the generosity of Dr. J. R. Brisson (NRC, Canada). This research was supported by NSF grants CHE-0518010 and NIH EY012347. NSF grants CHE0443516 and DBI0079461 provided funding for the 600 MHz NMR spectrometers used in this project.

Supporting Information Available: Experimental details, ^{1}H NMR, MALDI TOF-MS, IR, and ROESY spectra. This material is available free of charge via the Internet at http://pubs.acs.org.

JA808286X

(67) DeLano, W. L. DeLano Scientific LLC, Palo Alto, CA, 2007.
(68) Pettersen, E. F.; Goddard, T. D.; Huang, C. C.; Couch, G. S.; Greenblatt, D. M.; Meng, E. C.; Ferrin, T. E. *J. Comput. Chem.* **2004**, *25*, 1605–1612.